ASTRA Proc., 1, 51–60, 2014
www.astra-proceedings.net/1/51/2014/
doi:10.5194/ap-1-51-2014

ASTRA Proceedings Open Access

MHD flows at astropauses and in astrotails

D. H. Nickeler[1], T. Wiegelmann[2], M. Karlický[1], and M. Kraus[1]

[1]Astronomical Institute, AV ČR, Fričova 298, 25165 Ondřejov, Czech Republic
[2]Max-Planck-Institut für Sonnensystemforschung, Justus-von-Liebig-Weg 3, 37077 Göttingen, Germany

Correspondence to: D. H. Nickeler (dieter.nickeler@asu.cas.cz)

Received: 7 April 2014 – Revised: 14 August 2014 – Accepted: 19 August 2014 – Published: 5 September 2014

Abstract. The geometrical shapes and the physical properties of stellar wind – interstellar medium interaction regions form an important stage for studying stellar winds and their embedded magnetic fields as well as cosmic ray modulation. Our goal is to provide a proper representation and classification of counter-flow configurations and counter-flow interfaces in the frame of fluid theory. In addition we calculate flows and large-scale electromagnetic fields based on which the large-scale dynamics and its role as possible background for particle acceleration, e.g., in the form of anomalous cosmic rays, can be studied. We find that for the definition of the boundaries, which are determining the astropause shape, the number and location of magnetic null points and stagnation points is essential. Multiple separatrices can exist, forming a highly complex environment for the interstellar and stellar plasma. Furthermore, the formation of extended tail structures occur naturally, and their stretched field and streamlines provide surroundings and mechanisms for the acceleration of particles by field-aligned electric fields.

1 Introduction

When stars move through the interstellar medium (ISM), the material released via their winds collides and interacts with the ISM. This interaction produces several detectable structures, such as stellar wind bow shocks when stars move with supersonic speeds relativ to the ISM. Furthermore, a termination shock can form, where the supersonic stellar wind slows down to subsonic speed, and in between this termination shock and the outer bow shock a contact surface forms, separating the subsonic ISM flow from the subsonic stellar wind flow. This contact surface is called the astropause and has at least one stagnation point at which both flows, the stellar wind and the ISM material stop and diverge.

In downwind direction, a tail like structure can form, which is the astrotail. The tail is not only proposed by the result of simulations, but also by the fact that stretched field or streamlines minimize the corresponding tension forces, so that the configuration is able to approach an equilibrium state. Such bow shocks and astrotails have been directly observed, e.g., around asymptotic giant branch stars (e.g., Ueta, 2008; Sahai and Chronopoulos, 2010), and have been proposed to exist also around the Sun (e.g., Scherer and Fichtner, 2014).

Typically, a magnetic field is embedded in the ISM. For stars with a strong magnetic field, the wind is magnetized as well. Hence, different null points can appear, one of the flow and one of the magnetic field, which are not necessarily at the same location, unless the magnetic field is frozen-in (see, Nickeler and Karlický, 2008). The formation of a stagnation point of the flow or of a magnetic neutral point is crucial for the understanding how an interface in the form of an astropause forms between the very local ISM and a stellar wind. The best object to study counterflow configurations observationally is the heliosphere, where spacecrafts such as *Voyager 1* and *2* and *IBEX* perform in situ measurements of the plasma parameters (e.g., Burlaga et al., 2013; McComas et al., 2013; Fichtner et al., 2014). However, an interpretation of these observations is not always straight forward. While strong indications for the crossing of the termination shock of *Voyager 1* exist, it is yet unclear and contradictory whether the heliopause region was already left (Burlaga et al., 2013; Burlaga and Ness, 2014; Fisk and Gloeckler, 2013; Gurnett et al., 2013).

The problematics of computing counterflow configurations have been attacked from different viewpoints, such as hydrodynamics (see, e.g., Fahr and Neutsch, 1983b),

kinematical magnetohydrodynamics (MHD) (see, e.g., Suess and Nerney, 1990; Nerney et al., 1991, 1993, 1995), and self-consistent MHD (see, e.g., Neutsch and Fahr, 1982; Fahr and Neutsch, 1983a; Nickeler and Fahr, 2001, 2005, 2006; Nickeler et al., 2006; Nickeler and Karlický, 2006; Nickeler and Karlický, 2008), focusing on different aspects and regions within the astrosphere. We are aware that fluid approaches like MHD are strictly valid only for collisional plasmas, but are frequently applied to collisionless configurations like magnetospheres, coronae or astrospheres. The alternative approach, kinetic theory, is not applicable because of the difference of kinetic and macroscopic scales.

It is evident that numerical simulations allow to study more involved physical models (like full MHD), which cannot be solved analytically. On the other hand, the above cited analytical studies, including the present, have the advantage that they provide exact solutions, and they allow us to analyse physical and mathematical effects in great detail. In particular, analytical investigations are indispensable for studying how the distribution of the magnetic null points/stagnation points determines both the topology of the streamlines/magnetic field lines and the geometrical shape of the heliopause.

In this paper, we provide exact mathematical definitions of astrospheres and astropauses. We discuss possible shapes with respect to the spatial arrangement of the stagnation and/or null points and emphasize the role of the directions of flow and field of both the ISM and the star. Furthermore, we discuss the role of magnetic shear flows as possible trigger for particle acceleration (e.g., ACRs) in the heliotail.

2 Geometrical shapes and topological properties of astropauses

The geometrical shapes of astropauses depend on the strengths and directions of the two involved flows (stellar wind and ISM flow) and their electromagnetic fields. The fact that most of the ISM flow cannot penetrate the stellar wind region but is forced to flow around defines the boundary called astropause. In the mathematical sense, the streamlines in the local ISM and in the stellar wind region are topologically disjoint. Still, different possibilities for the definition of the physical astropause exist. One way to define the location of this boundary might be to use the stagnation point of the flow as criterion. This stagnation point is the intersection of the stagnation line and the astropause (separatrix) surface. The stagnation line is this streamline along which all fluid elements heading towards the astropause and coming from opposite directions, i.e., on the one hand from the ISM and on the other hand from the star, are decelerated down to zero velocity. However, such a definition is only useful in a single-fluid (i.e., classical HD or MHD) theory, while in a more general multi-fluid model different pauses (i.e., one for each component) exist. Here a definition via a stagnation point of the flow is not unique. A precise way is thus to use the null point of the magnetic field, and to transfer the concept of the stagnation point of the flow to the magnetic field configuration. Such a definition via the null point of the magnetic field makes only sense as long as the star itself has a magnetic field, strong enough to be dynamically important. Here, we focus on stars with magnetic fields, for which the astropause can be uniquely defined as the outermost magnetic separatrix. The most well-known magetic star is our Sun with its boundary, the heliopause.

2.1 Definition of a separatrix

The field lines of a vector field are typically represented by the trajectories of a corresponding system of ordinary differential equations, the so-called phase portrait. Physically interesting phase portraits are those in which null points exist. Then, a topological classification of the local vector field can be performed by analysing the eigenvalues of the corresponding Jacobian matrix of the vector field at the null point (see, e.g., Lau and Finn, 1990; Arnol'd, 1992; Parnell et al., 1996). The configuration of the vector field in the vicinity of the magnetic null point depends on the dimension of the considered problem. For instance, in 3-D, the magnetic null point is the intersection of the 1-D stable or unstable submanifold termed the spine, with a 2-D unstable or stable manifold termed the fan. This 2-D manifold is termed the separatrix (or pause). In cartesian 2-D, the magnetic null point is the intersection of two separatrix field lines of which one is called stable and the other one is called unstable. This null point in 2-D is of X-point type. Trajectories, i.e., streamlines or field lines, of the vector field are called stable, when the streamline or field line points towards the null point, while they are called unstable when they point away from the null point. Such configurations can only be obtained if the eigenvalues of the Jacobian matrix of the vector field at the null point are of so-called hyperbolic or saddle point type. More specifically, in 2-D the eigenvalues are real and have opposite signs, while in 3-D the situation is more complex. Here, the real parts of the eigenvalues should not vanish and always two of their real parts have the identical sign. Basically, this separatrix concept is valid also concerning the flow field in HD or MHD.

The definition of a separatrix was so far only restricted to a scenario with a single, isolated null point. In real astrophysical scenarios, multiple null points may exist, depending on the complexity of the stellar wind and its magnetic field. Therefore, multiple and highly complex, maybe even nested separatrices may occur. For instance, Swisdak et al. (2013) find that the heliopause can be considered as a region consisting of bundles of separatrices and magnetic islands, resulting from magnetic reconnection processes, which form a porous, multi-layered structure. Examples of multiple and nested separatrices originating from X-type null points are shown and discussed in the following.

2.2 Determination of the global shape of astrospheres: distribution of null points for pure potential fields

To compute non-linear MHD flows with separatrices as we will do in Sect. 3, geometrical patterns are needed for the structure of the corresponding flows and fields. To obtain such patterns, we start from the simplest possible fields, the potential fields, and investigate how separatrices form and how they are shaped by different spatial distributions of null points. The advantage of using potential fields is given by the fact that these fields obey a superposition principle, i.e., they are linear, and every null point is automatically an X-point of the magnetic field. In addition, potential fields have no free magnetic energy (i.e., they are stable) and can easily be mapped to non-linear fields by either generalized contact transformations or algebraic transformations. The concept of contact transformations was presented, e.g., by Gebhardt and Kiessling (1992) and later on used and refined by Nickeler and Wiegelmann (2010, 2012); Nickeler et al. (2006, 2013) to describe the MHD fields of different space plasma environments, while the algebraic transformations were introduced by Bogoyavlenskij (2000a, b, 2001, 2002).

As was shown by Fahr et al. (1993) in the case of pure HD and by Nickeler et al. (2006) in the case of MHD, the number and spatial distribution of the hyperbolic null points determine the topological scaffold of an astrosphere. This, in combination with the assumption of a homogeneous background field as asymptotic boundary condition, allows us to describe the general shape of its field and streamlines. In the current paper, we aim at giving a qualitative overview of the different scenarios. For the detailed theoretical description and treatment we refer to Nickeler et al. (2006).

If several hyperbolic null points exist, which of the separatrices defines then the real pause? What can be said about multiple null points is that they all have to be non-degenerate, because double or higher order null points are topologically unstable (e.g., Hornig and Schindler, 1996).

Having discussed the general topological aspects, we now focus on the geometrical ones, considering a simplified 2-D scenario, in analogy to typical flows in aero and fluid dynamics. While in the vicinity of the star the fields are full 2-D to account for a variety of multipolar field structures, asymptotically, i.e., far away from the star in downwind direction, the field converges to a tail-like (1-D) structure. Let us start with the case of two null points in the frame of a 2-D cartesian potential field. We assume that the z direction is the invariant direction, which means that for all parameters $\partial/\partial z = 0$. Further, x points to the downwind (i.e. tail) direction, and y in perpendicular direction. The global magnetic field, $\boldsymbol{B} = \nabla A(x,y) \times \boldsymbol{e}_z$, with the unit vector $\boldsymbol{e}_z$ in z direction, can be described via complex analysis. As $\boldsymbol{B}$ should be a potential field, it follows that $\Delta A = 0$. To solve this Laplace equation, we define a stream or, here, the magnetic flux function A by $A = \Im(\mathcal{A})$, where $\mathcal{A}$ is the complex stream or magnetic flux function. This complex flux function is obtained from a Laurent series of the form (see, e.g., Nickeler et al., 2006)

$$\mathcal{A} = B_{S\infty} u + C_0 \ln u + \frac{C_1}{u} + \text{terms of higher order}. \qquad (1)$$

In the following, we will neglect the higher order terms, so that the complex magnetic flux function consists purely of a monopole[1] and a dipole. Both multipoles are located in the origin. Here, $u = x + iy$ is the complex coordinate, $B_{S\infty}$ is the asymptotical boundary condition $\lim B = B_{S\infty}$ for $|u| \to \infty$, i.e., the background field, and C_0 and C_1 are the monopole and dipole moments, respectively. For the case of two null points, these moments have the following form

$$C_0 = -B_{S\infty}(u_1 + u_2) \text{ and } C_1 = -B_{S\infty} u_1 u_2, \qquad (2)$$

where u_1 and u_2 are the complex coordinates of the two null points.

The simplest scenario is the one with two symmetric null points ($u_1 = -u_2$). In this case, only the dipole moment exists, and we can interprete this with a star with a dipole magnetic field embedded in a homogeneous magnetic background field. Such a scenario is an analogy to the classical hydrodynamical example of a cylindrical obstacle in a homogeneous flow. If we assume the star is located at the origin of a cartesian coordinate system and the flow is parallel to the x axis and streams in positive x direction, the separatrices form a circle in the (x, y) plane, where the stagnation lines lie on the x axis and intersect the circular separatrix from both sides at the two null points and pass through the pole. This is shown in the upper left panel of Fig. 1. The radius R of the circular separatrix, and hence the location of the two symmetric null points, depends on the strength of the background magnetic field ($B_{S\infty}$) and the dipole field via $R^2 = B_0 R_0^2 / B_{S\infty}$. The term $B_0 R_0^2$ is hereby the dipole moment. Such a symmetric scenario is not very realistic, because it would imply a completely closed separatrix. Hence, no plasma can escape via the stellar wind.

To enable at least a half-open astrosphere, the second null point (the one in the downwind region) must be located closer to the pole. The shape of the resulting separatrices for different pole distances are depicted in the series of plots in Fig. 1. When moving the second null point towards the pole, one can notice several effects. First, the separatrix resulting from the first null point "opens" in the downwind region. Second, an inner, closed separatrix is formed that passes through the second null point and through the pole. This separatrix encloses now the dipolar field region, which became smaller, and the dipole field weaker, if the same background field is present. This inner separatrix meets the stagnation line from the first null point at the pole. A measurable bundle

[1] The monopole is introduced as a mathematical tool, used to generate radial streamlines (i.e. the stellar wind) and radial (i.e. open) field lines. Without it, the streamlines and magnetic field lines would otherwise always be closed.

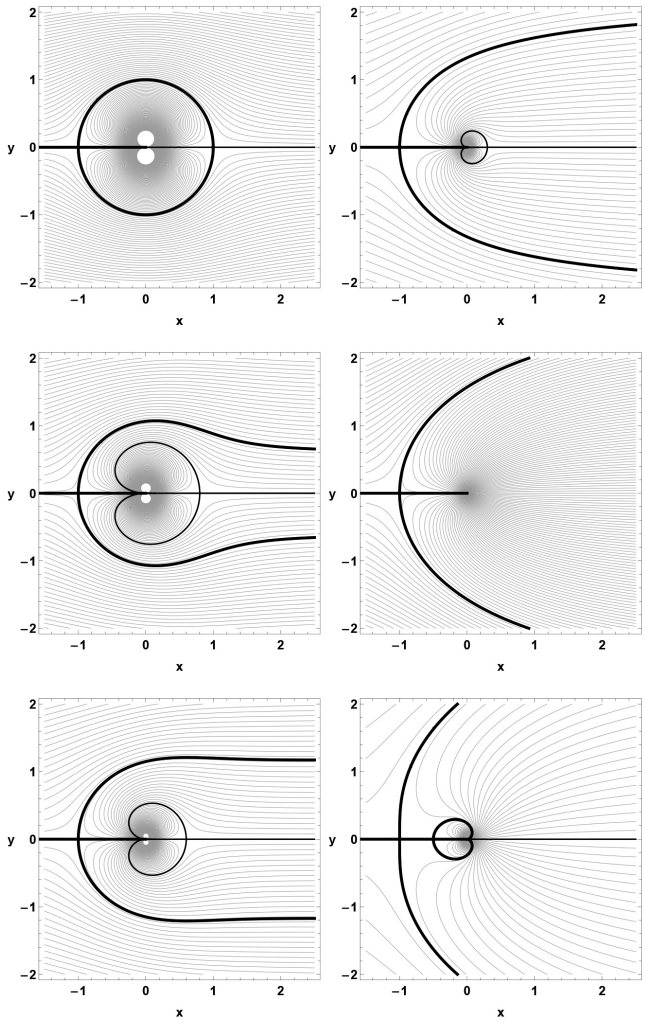

Figure 1. Shape of the separatrices in dimensionless units for the case of two null points lying on the x axis. Shown are the field lines (i.e., the projection of the contour lines of A into the x–y plane). One null point is fixed at $u_1 = x = -1$, the other one, u_2, is at $x = 1$ (symmetric, left top), $x = 0.8$ (left middle), $x = 0.6$ (left bottom), $x = 0.3$ (right top), $x = 0$ (Parker scenario, right middle), $x = -0.5$ (right bottom). In the Parker scenario, the second null point disappears (coincides with the pole) and therefore also the dipole moment. The separatrices defined by u_1 are plotted with strongest, those defined by u_2 with medium, and field lines are shown with normal line width.

of field lines can leave the inner dipole region upstream, i.e., between the inner separatrix and the stagnation line. These field lines origin from the monopole part of the field. They are deflected at the outer separatrix so that they bend around the inner separatrix and extend as open field lines into the astrotail, forming the inner astrosheath field lines. The closer the second null point is located to the pole, the more opens the tail region.

As soon as the second null point "reaches" the pole, it vanishes. Hence, only one real null point remains and the field has only a monopole moment. This scene is shown in the middle right panel of Fig. 1 and is similar to the Parker scenario (Parker, 1961) for subsonic flows. If the second null point is located on the same side as the first one, i.e., in upwind direction (lower right panel of Fig. 1), the second separatrix is also located in upwind direction and both null points are physically connected by the stagnation line. In addition, the monopole moment increases so that the astrotail becomes even wider.

Restricting for the moment to a single null point, it is, of course, not necessary that this null point is located on the x axis. For instance, with respect to the heliopause, measurements from *Voyager 1* indicate an asymmetry (Burlaga et al., 2013). A natural way to displace the null point is provided by the solar (or stellar, in general) rotation, which results in a winding-up of the field lines and hence to a spiral structure of the magnetic field. While the monopole moment in the symmetric examples is a pure real number, it now becomes complex. Hence, an azimuthal component of the outflow or field occurs. The result is a displacement of the null point off the x axis. This is demonstrated in Fig. 2, where we plot the asymmetric configuration[2] in comparison to the symmetric one. An even more complex situation is achieved when a second null point exists in the asymmetric scene. Such an example is shown in Fig. 3.

Having multiple, nested separatrices, the real astropause can be uniquely defined by the outermost magnetic separatrix between the magnetized interstellar medium and the magnetized stellar wind.

3 Self-consistent non-linear MHD flows

The pattern of the potential fields, as we calculated in the previous section, serve now as static MHD equilibria (MHS). These are then mapped with the non-canonical transformation method to self-consistent steady-state MHD flows. Thereby we make use of estimated or observed physical quantities, such as density, magnetic field strength, etc., within and outside the heliosphere. These quantities serve as asymptotical boundary conditions, based on which some of the coefficients of the mapping can be fixed.

Observations from *Voyager 1* suggest that the plasma flow in the vicinity of the heliopause and in the heliotail region is approximately parallel to the magnetic field (Burlaga et al., 2013; Fisk and Gloeckler, 2013). In addition, the plasma within a stagnation region is incompressible. This can be understood in terms of the steady-state mass

[2]Considering that *Voyager 1* might have passed the stagnation region at a distance of 123 AU (Krimigis et al., 2013), meaning that within our scenario u_1 would be at roughly 123 AU, our configuration shown in Fig. 2 (bottom) and Fig. 3 might be approximately scaled with 1 : 87 AU.

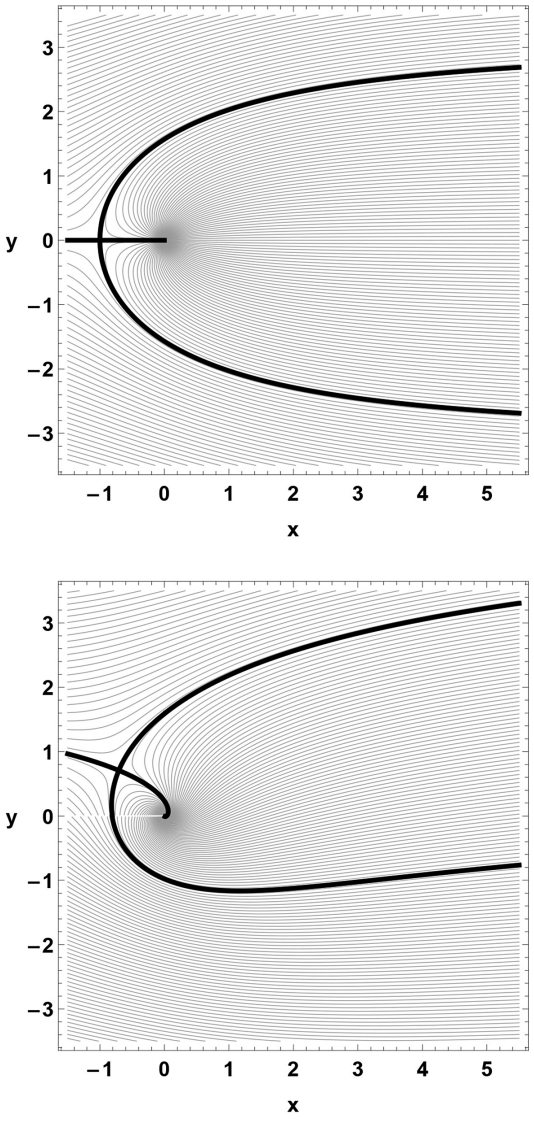

Figure 2. As Fig. 1, but comparing separatrix shapes with only one null point. Top: the symmetric Parker case ($u_1 = x = -1$), and bottom: the asymmetric case where u_1 is rotated off the x axis by $-\pi/4$, i.e., $u_1 = -1(\cos(-\pi/4) + i\sin(-\pi/4))$. The apparent non-connectivity of some field lines at $y = 0$ and $x < 0$ is not real but caused by the flip between Riemann surfaces.

continuity equation

$$\nabla \cdot (\rho\, \boldsymbol{v}) = 0 \quad \Leftrightarrow \quad \boldsymbol{v} \cdot \nabla \rho + \rho \nabla \cdot \boldsymbol{v} = 0\,. \tag{3}$$

When approaching the stagnation point, i.e. $\boldsymbol{v} \to \boldsymbol{0}$, the term $\boldsymbol{v} \cdot \nabla \rho$ in the second equation vanishes, implying that $\rho \nabla \cdot \boldsymbol{v}$, and in particular, as the density reaches a maximum, $\nabla \cdot \boldsymbol{v}$ has to vanish as well.[3] The plasma flow on streamlines, which originate in such stagnation point regions, transports

[3]This remains valid, even if $\nabla \rho$ happens to become extremely large across the heliopause boundary layer.

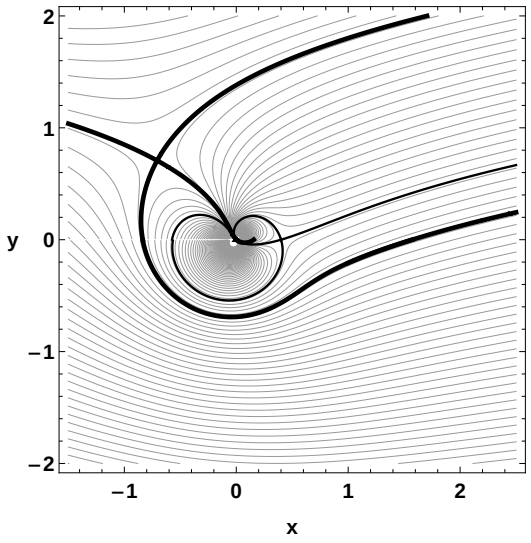

Figure 3. As Fig. 1, but for an asymmetric case where the front null point is rotated off the x axis by $-\pi/4$, i.e., $u_1 = -1(\cos(-\pi/4) + i\sin(-\pi/4))$, and the other one is on the x axis at $u_2 = x = 0.4$. The apparent non-connectivity of some field lines at $y = 0$ and $x < 0$ is not real but caused by the flip between Riemann surfaces.

the property of incompressibility further into the tail region. Hence, it is reasonable to investigate the heliotail and heliopause region using field-aligned, incompressible flows, and the basic ideal MHD equations are given by

$$\nabla \cdot (\rho \boldsymbol{v}) = 0\,, \tag{4}$$
$$\rho\, (\boldsymbol{v} \cdot \nabla)\, \boldsymbol{v} = \boldsymbol{j} \times \boldsymbol{B} - \nabla p\,, \tag{5}$$
$$\nabla \times (\boldsymbol{v} \times \boldsymbol{B}) = \boldsymbol{0}\,, \tag{6}$$
$$\nabla \times \boldsymbol{B} = \mu_0 \boldsymbol{j}\,, \tag{7}$$
$$\nabla \cdot \boldsymbol{B} = 0\,, \tag{8}$$
$$\nabla \cdot \boldsymbol{v} = 0\,, \tag{9}$$
$$\boldsymbol{v} = \pm |M_A| \boldsymbol{v}_A \tag{10}$$
$$\boldsymbol{v}_A := \frac{\boldsymbol{B}}{\sqrt{\mu_0 \rho}}\,, \tag{11}$$

where ρ is the mass density, $\boldsymbol{v}$ is the plasma velocity, $\boldsymbol{B}$ is the magnetic flux density, $\boldsymbol{j}$ is the current density, p is the plasma pressure, M_A is the Alfvén Mach number, $\boldsymbol{v}_A$ is the Alfvén velocity, and μ_0 is the magnetic permeability of the vacuum.

Given solutions for p_S and B_S of the MHS equations

$$\nabla p_S = \boldsymbol{j}_S \times \boldsymbol{B}_S\,, \tag{12}$$

and additional solutions for M_A and ρ of the systems

$$\boldsymbol{B}_S \cdot \nabla \rho = 0\,, \tag{13}$$
$$\boldsymbol{B}_S \cdot \nabla M_A = 0\,, \tag{14}$$

are the parameters needed to perform the transformation, i.e.,

to compute the general solution (see, e.g., Nickeler and Wiegelmann, 2012) of the system Eq. (4)–(11)

$$\boldsymbol{B} = \frac{\boldsymbol{B}_\mathrm{S}}{\sqrt{1-M_A^2}}, \tag{15}$$

$$p = p_\mathrm{S} - \frac{1}{2\mu_0}\frac{M_A^2\,|\boldsymbol{B}_\mathrm{S}|^2}{1-M_A^2}, \tag{16}$$

$$\sqrt{\rho}\boldsymbol{v} = \frac{1}{\sqrt{\mu_0}}\frac{M_A\boldsymbol{B}_\mathrm{S}}{\sqrt{1-M_A^2}}, \tag{17}$$

$$\boldsymbol{j} = \frac{M_A}{\mu_0}\frac{\nabla M_A \times \boldsymbol{B}_\mathrm{S}}{\left(1-M_A^2\right)^{\frac{3}{2}}} + \frac{\boldsymbol{j}_\mathrm{S}}{\left(1-M_A^2\right)^{\frac{1}{2}}}. \tag{18}$$

Properties of these solutions are that the plasma density ρ, the Alfvén Mach number M_A, and the Bernoulli-pressure $p+\frac{1}{2}\boldsymbol{v}^2$ are constant on field lines. However, these parameters can vary perpendicular to the field lines, which means that for example strong shear flows, implying a strong gradient of the Alfvén Mach number, produce strong current densities (curent sheets). This is obvious from Eq. (18), even if we start from a potential field, which implies $\boldsymbol{j}_\mathrm{S} = \boldsymbol{0}$. The occurrence of current sheets, especially around multiple separatrices, is known, e.g., in solar flare physics, as current fragmentation (e.g., Karlický and Bárta, 2008a, b; Bárta et al., 2010), or, in steady-state as fragmented currents (e.g., Nickeler et al., 2013). It should be emphasized that a similar transformation can also be performed using super-Alfvénic flows.

In the following, we concentrate on the tail region, taking the symmetric Parker-like tail (top panel of Fig. 2). The mapping ansatz we use was described in detail in Nickeler et al. (2006). The Alfvén Mach number is defined via $M_A^2 = 1-1/(\alpha'(A))^2$, where the prime denotes the derivation with respect to A, and α is the mapped z component of the vector potential of A. This means that if $\boldsymbol{B}_\mathrm{S} = \nabla A \times \boldsymbol{e}_z$ and $\alpha = \alpha(A)$, then $\boldsymbol{B} = \nabla\alpha(A)\times\boldsymbol{e}_z = \alpha'(A)\nabla A\times\boldsymbol{e}_z$. Hence, $\alpha'(A)$ is the amplification factor for the magnetic field strength, and it results to

$$\alpha'(A) = \frac{1}{2}\left(\frac{1}{\sqrt{1-M_{A\infty}^2}} - \frac{1}{\sqrt{1-M_{A,i}^2}}\right) \cdot \left(\tanh\frac{\frac{A}{\sqrt{1-M_{A\infty}^2}B_\infty} - y_1}{d_1} - \tanh\frac{\frac{A}{\sqrt{1-M_{A\infty}^2}B_\infty} + y_1}{d_1}\right). \tag{19}$$

The ansatz for $\alpha'(A)$ is chosen in order to mimic two current sheets located symmetrically at $\pm y_1$ around the heliopause field lines, with oppositely directed currents. To compute the Mach number profile and the current sheets, we use the following set of values (see, e.g. Frisch et al., 2012; Burlaga et al., 2013): for the magnetic field of the interstellar medium $B_\infty = 5\,\mu\mathrm{G}$, for the inner magnetic field strength in the tail $B_\mathrm{i} = 4\,\mu\mathrm{G}$, the particle number densities of electrons and ions are about equal and $n_\mathrm{e} \approx n_\mathrm{i} = 0.1\,\mathrm{cm}^{-3}$, the velocity of the ISM plasma relative to the sun is $v_\infty = 25\,\mathrm{km\,s}^{-1}$, and the Mach numbers of the ISM plasma and of the heliotail result to $M_{A\infty} = 0.72$ and $M_{A,i} = 0.52$. These values might not be absolutely true, but they are used here to provide a rough idea of the global shape of the current sheets.

The Alfvén Mach number profile for the chosen parameters is shown in the top panel of Fig. 4. It is computed for a thickness of the current sheets in the tail of $d_1 = 100\,\mathrm{AU}$. This is an unrealistic scenario, and is only shown to highlight the current distribution in the tail (middle panel of Fig. 4). A more realistic case for the current sheets requires much narrower widths. This is depicted in the lower panel of Fig. 4 where we use a width of only 10 AU. Obviously, a reduction in the width by a factor of ten leads to an increase of the current strength by a factor of ten. At the boundary between ISM and solar wind flows, Kelvin–Helmholtz-like or current driven reconnection instabilities can occur due to shear flows and extremely high current densities, respectively. These instability regions are thus ideal locations for plasma heating and particle acceleration.

4 Magnetic shear as trigger for particle acceleration

The separatrix regions and, in particular, the heliotail regions can serve as important particle acceleration locations. This assumption is supported by observations of both the cosmic ray anisotropy and the broad excess of sub-TeV cosmic rays in the direction of the heliotail. Lazarian and Desiati (2010) propose that this excess originates from magnetic reconnection in the magnetotail. The heliotail/heliopause region was also considered by Lazarian and Opher (2009) as an important region for particle acceleration. In their approach, Lazarian and Opher (2009) use a Spitzer-like resistivity and propose first-order Fermi acceleration as the dominant acceleration process of energetic particles along the magnetotail. In contrast, to approach the problematics of particle acceleration we focus on the magnetic shear generated by magnetic shear flows across the heliopause boundary. To reduce the complexity of the problem, we shear here the magnetic field only in z direction. This guarantees that the current, and, therefore, also the electric field, are aligned with the tail direction.

We investigate the generation of parallel electric fields and consider them as acceleration engines which, in solar physics, is typically referred to as direct current (DC) field acceleration (see, e.g., Aschwanden, 2002). The link to solar physics scenarios is obvious, as the acceleration process takes place in a diluted plasma environment, i.e., in regions of low density.

As the magnetic field jumps across the heliopause, the magnetic shear in z direction, B_z, is connected with a narrow current sheet located around the heliopause and extending into the heliotail. As in the tail region the flow is directed

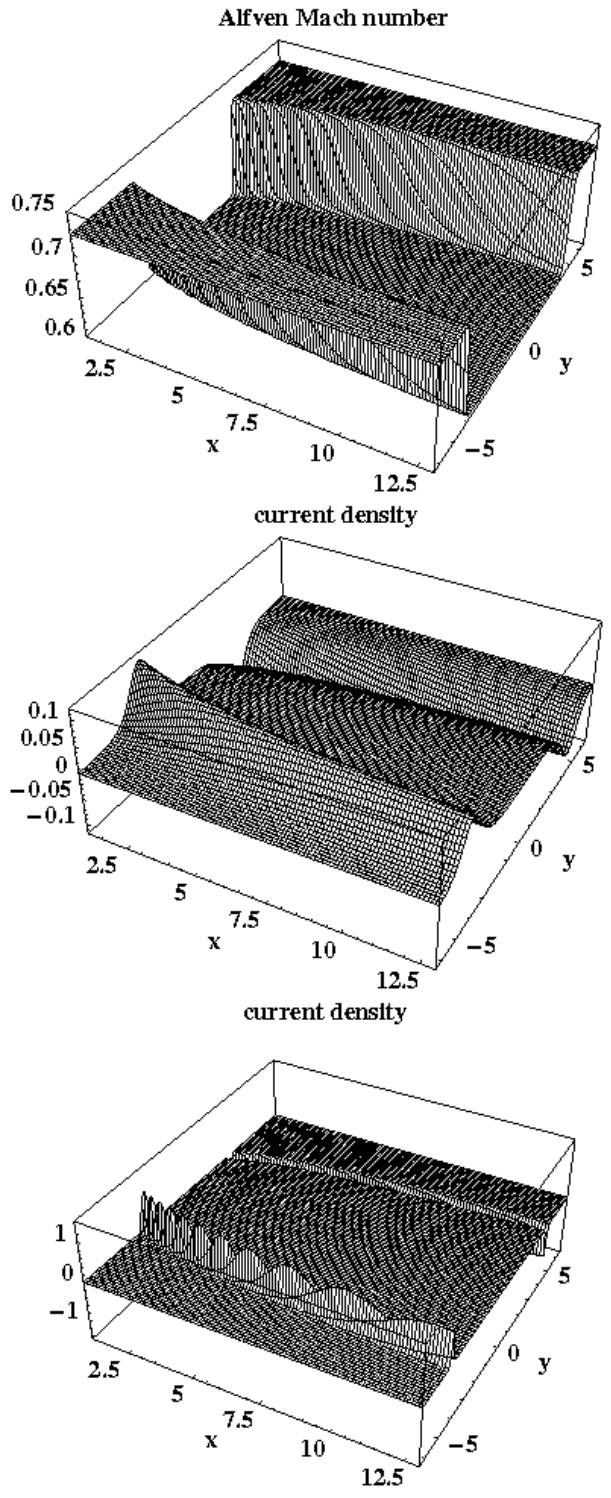

Figure 4. Alfvén Mach number profile (top, restricted to $M_A > 0.6$ for displaying purposes) and resulting current sheets for a sheet width of 100 AU (middle) and 10 AU (bottom). The current density of the poloidal magnetic field is here given in units of 2.65×10^{-17} A m^{-2}.

along the field lines, the presence of a current density immediately implies that even in such a field-aligned flow scenario an electric field can exist due to the validity of resistive Ohm's law $\boldsymbol{E} + \boldsymbol{v} \times \boldsymbol{B} = \eta \boldsymbol{j}$, as long as the resistivity $\eta \neq 0$. Furthermore, as was shown by Nickeler et al. (2014), the solution of non-ideal Ohm's law decouples from the rest of the MHD equations as the flow is field-aligned. Therefore, the only additional equation to be solved is

$$\nabla \times (\eta \boldsymbol{j}) = \boldsymbol{0}\,, \tag{20}$$

as $\boldsymbol{E} = \eta \boldsymbol{j}$ and $\nabla \times \boldsymbol{E} = \boldsymbol{0}$ (stationary approximation).

A reasonable resistivity should be valid in our steady-state model and account for the case of a collisionless plasma. While the Spitzer resistivity is effective only in collisional plasmas, the turbulent collisonless resistivity (anomalous resistivity due to wave-particle interactions) is usually not stationary.

The usual approach for the resistivity is to use the electric force and to introduce some frictional force νv_D acting on the charges q, with the collision frequency ν and the drift velocity v_D (e.g. Papadopoulos, 1977)

$$\frac{\mathrm{d}v_\mathrm{D}}{\mathrm{d}t} = \frac{q}{m}E - \nu v_\mathrm{D} = 0 \quad \wedge \quad E = \eta j = \eta n q v_\mathrm{D} \tag{21}$$

$$\Rightarrow \quad \eta = \frac{m\nu}{nq^2}\,. \tag{22}$$

For our collisionless plasma, we consider the interaction between the electromagnetic field and charged particles as a substitute for collisions. This ansatz is motivated by the fact that the interaction time, which is limited by the time the particle needs to cross the current sheet, i.e. the "transit time" of the particle within the system, is much shorter than the collision time. Hence the collision time (collision frequency ν) has to be replaced by the gyro-time (gyro-frequency qB/m), delivering

$$\eta = \frac{1}{\sigma_\mathrm{g}} \quad \text{with} \quad \sigma_\mathrm{g} = \frac{nq}{|\boldsymbol{B}|}\,, \tag{23}$$

where σ_g is the gyroconductivity, n and q are the particle number density and charge, respectively. This approach was introduced by Speiser (1970) and Lyons and Speiser (1985) and the resulting resistivity is called inertial or gyro-resistivity. We want to emphasize that the substitution of the collision frequency by the gyro-frequency automatically delivers huge resistivity values in the case of a diluted plasma, which are only important for the generation of an electric field in regions of strong current density and not in regions where the field has the character of a potential field.

We use an approximate value for the magnetic shear of $B_z \approx 10^{-11}$ T, which is of the order of 10 % of the heliotail (or ISM) magnetic field strength and can be regarded as a lower bound. For the typical lengthscale of the shear layer we set $l \approx 10^3$ km (e.g., Fahr and Neutsch, 1983a). Hence,

we can estimate the resulting current density via

$$|\boldsymbol{j}| \approx \frac{|B_z|}{\mu_0 l} = 5.3 \times 10^{-11}\,\mathrm{A\,m^{-2}}. \quad (24)$$

For density values of $10^4\,\mathrm{m^{-3}}$ (Fahr et al., 1986) and magnetic field strengths of $2 \times 10^{-10}\,\mathrm{T}$ typical for heliotail conditions, the gyroresisitivity η is on the order of $10^5\,\mathrm{Ohm\,m}$. Consequently, the parallel electric field becomes

$$E_\parallel = \frac{\boldsymbol{E}\cdot\boldsymbol{B}}{|\boldsymbol{B}|} \approx \frac{\eta}{\mu_0}|\boldsymbol{j}| \approx 10^{-6}\,\mathrm{V\,m^{-1}}. \quad (25)$$

Within the tail, the field lines are stretched, and the current is concentrated around the heliopause region, providing a sufficiently extended environment for accelerating particles continuously along the magnetic field lines. Outside this narrow region, the current vanishes and hence also the electric field, so that those astrosphere regions can be ideal.

Considering a relatively conservative case, in which the field aligned electric field extends to about 100 AU, only, meaning that the tail extends to just twice the distance than the heliopause nose, the voltage seen by the particles is

$$\int E_\parallel \mathrm{d}s \approx E_\parallel \cdot s \approx 10^7\,\mathrm{V}. \quad (26)$$

This voltage can contribute to cosmic ray acceleration.

5 Discussion and conclusions

We have shown that the distribution of null points and stagnation points defines the global topology and the large-scale structure of an astrosphere. Multiple separatrices can exist implying jumps (tangential discontinuities) of several physical parameters, such as the magnetic field strength, particle density, etc. As the outermost separatrix defines the astropause, its global geometrical shape is hence also determined.

With respect to the heliosphere, the multiple decreases and increases in the magnetic field strength as well as in other physical parameters measured by *Voyager 1* (Burlaga et al., 2013) indicates several crossings of either one or several individual separatrices. Such a scenario is in good qualitative agreement with the multiple separatrix structures due to more than one null point as proposed here and formerly by Nickeler et al. (2006). A similar scene considering multiple, nested separatrices and magnetic islands was recently suggested based on detailed numerical simulations by Swisdak et al. (2013).

Interestingly, our results for the two null point scenarios also agree with the recently proposed presence of a heliocliff region inside the heliopause (Fisk and Gloeckler, 2013). In particular, the heliocliff might be interpreted as the separatrix resulting from the second null point (as shown in the middle left panel of Fig. 1), and the streamlines originating from the monopole part, which bend into the heliotail, would represent the open heliosheath as introduced by Fisk and Gloeckler (2013). In the heliocliff region, the model of Fisk and Gloeckler (2013) turns out to produce a super-Alfvénic field-aligned flow, while in our model the flow close to the heliopause and in the heliotail region is field-aligned but can also be sub-Alfvénic.

Furthermore, the presence of magnetic shear flows can produce vortex current sheets (Nickeler and Wiegelmann, 2012) leading to the generation of instabilities and magnetic reconnection close to separatrices. In the current work we restrict our analysis to a maximum of two separatrices and we apply the mapping only to the heliotail with one symmetric separatrix (top panel of Fig. 2) with two current sheets. As multiple separatrices can exist in the heliosphere, the presence of multiple curent sheets in the vicinity of these separatrices can lead to fragmented structures (e.g., Nickeler et al., 2013; Swisdak et al., 2013). Introducing a non-collisional resistivity, strong electric (DC) fields parallel to the magnetic field can be generated, which can contribute to cosmic ray acceleration as suggested by Nickeler (2005).

Acknowledgements. We thank Andreas Kopp and two more, anonymous referees for helpful comments on the paper draft. This research made use of the NASA Astrophysics Data System (ADS). D. H. Nickeler and M. Karlický acknowledge financial support from GA ČR under grant numbers 13-24782S and P209/12/0103, respectively. The Astronomical Institute Ondřejov is supported by the project RVO:67985815.

Edited by: H. Fichtner
Reviewed by: A. Kopp and two anonymous referees

References

Arnol'd, V. I.: Ordinary Differential Equations, Springer-Verlag, Berlin Heidelberg New York, 1992.

Aschwanden, M. J.: Particle acceleration and kinematics in solar flares – A Synthesis of Recent Observations and Theoretical Concepts, Space Sci. Rev., 101, 1–227, 2002.

Bárta, M., Büchner, J., and Karlický, M.: Multi-scale MHD approach to the current sheet filamentation in solar coronal reconnection, Adv. Space Res., 45, 10–17, 2010.

Bogoyavlenskij, O. I.: Counterexamples to Parker's theorem, J. Math Phys., 41, 2043–2057, 2000a.

Bogoyavlenskij, O. I.: Helically symmetric astrophysical jets, Phys. Rev. E, 62, 8616–8627, 2000b.

Bogoyavlenskij, O. I.: Infinite symmetries of the ideal MHD equilibrium equations, Phys. Lett. A, 291, 256–264, 2001.

Bogoyavlenskij, O. I.: Symmetry transforms for ideal magnetohydrodynamics equilibria, Phys. Rev. E, 66, 056410, doi:10.1103/PhysRevE.66.056410, 2002.

Burlaga, L. F. and Ness, N. F.: *Voyager 1* Observations of the Interstellar Magnetic Field and the Transition from the Heliosheath, Astrophys. J., 784, 146, doi:10.1088/0004-637X/784/2/146, 2014.

Burlaga, L. F., Ness, N. F., and Stone, E. C.: Magnetic Field Observations as Voyager 1 Entered the Heliosheath Depletion Region, Science, 341, 147–150, 2013.

Fahr, H. J. and Neutsch, W.: Stationary plasma-field equilibrium states in astropause boundary layers. I – General theory, Mon. Not. R. Astron. Soc., 205, 839–857, 1983a.

Fahr, H. J. and Neutsch, W.: Pressure distribution at the inner boundary of an astropause caused by a compressible stellar wind, Astron. Astrophys., 118, 57–65, 1983b.

Fahr, H. J., Neutsch, W., Grzedzielski, S., Macek, W., and Ratkiewicz-Landowska, R.: Plasma transport across the heliopause, Space Sci. Rev., 43, 329–381, 1986.

Fahr, H.-J., Fichtner, H., and Scherer, K.: Determination of the heliospheric shock and of the supersonic solar wind geometry by means of the interstellar wind parameters, Astron. Astrophys., 277, 249–264, 1993.

Fichtner, H., Scherer, K., Effenberger, F., Zönnchen, J., Schwadron, N., and McComas, D. J.: The IBEX ribbon as a signature of the inhomogeneity of the local interstellar medium, Astron. Astrophys., 561, A74, doi:10.1051/0004-6361/201322064, 2014.

Fisk, L. A. and Gloeckler, G.: The Global Configuration of the Heliosheath Inferred from Recent *Voyager 1* Observations, Astrophys. J., 776, 79, doi:10.1088/0004-637X/776/2/79, 2013.

Frisch, P. C., Andersson, B.-G., Berdyugin, A., Piirola, V., DeMajistre, R., Funsten, H. O., Magalhaes, A. M., Seriacopi, D. B., McComas, D. J., Schwadron, N. A., Slavin, J. D., and Wiktorowicz, S. J.: The Interstellar Magnetic Field Close to the Sun. II., Astrophys. J., 760, 106, doi:10.1088/0004-637X/760/2/106, 2012.

Gebhardt, U. and Kiessling, M.: The structure of ideal magnetohydrodynamics with incompressible steady flow, Phys. Fluids B-Plasma, 4, 1689–1701, 1992.

Gurnett, D. A., Kurth, W. S., Burlaga, L. F., and Ness, N. F.: In Situ Observations of Interstellar Plasma with Voyager 1, Science, 341, 1489–1492, 2013.

Hornig, G. and Schindler, K.: Magnetic topology and the problem of its invariant definition, Phys. Plasmas, 3, 781–791, 1996.

Karlický, M. and Bárta, M.: Fragmentation of Current Sheet, Central European Astrophysical Bulletin, 32, 35–38, 2008a.

Karlický, M. and Bárta, M.: Fragmentation of the Current Sheet, Anomalous Resistivity, and Acceleration of Particles, Sol. Phys., 247, 335–342, 2008b.

Krimigis, S. M., Decker, R. B., Roelof, E. C., Hill, M. E., Armstrong, T. P., Gloeckler, G., Hamilton, D. C., and Lanzerotti, L. J.: Search for the Exit: Voyager 1 at Heliosphere's Border with the Galaxy, Science, 341, 144–147, 2013.

Lau, Y.-T. and Finn, J. M.: Three-dimensional kinematic reconnection in the presence of field nulls and closed field lines, Astrophys. J., 350, 672–691, 1990.

Lazarian, A. and Desiati, P.: Magnetic Reconnection as the Cause of Cosmic Ray Excess from the Heliospheric Tail, Astrophys. J., 722, 188–196, 2010.

Lazarian, A. and Opher, M.: A Model of Acceleration of Anomalous Cosmic Rays by Reconnection in the Heliosheath, Astrophys. J., 703, 8–21, 2009.

Lyons, L. R. and Speiser, T. W.: Ohm's law for a current sheet, J. Geophys. Res., 90, 8543–8546, 1985.

McComas, D. J., Dayeh, M. A., Funsten, H. O., Livadiotis, G. and Schwadron, N. A.: The Heliotail Revealed by the *Interstellar Boundary Explorer*, Astrophys. J., 771, 77, doi:10.1088/0004-637X/771/2/77, 2013.

Nerney, S., Suess, S. T., and Schmahl, E. J.: Flow downstream of the heliospheric terminal shock – Magnetic field kinematics, Astron. Astrophys., 250, 556–564, 1991.

Nerney, S., Suess, S. T., and Schmahl, E. J.: Flow downstream of the heliospheric terminal shock - The magnetic field on the heliopause, J. Geophys. Res., 98, 15169–15176, doi:10.1029/93JA01177, 1993.

Nerney, S., Suess, S. T., and Schmahl, E. J.: Flow downstream of the heliospheric terminal shock: Magnetic field line topology and solar cycle imprint, J. Geophys. Res., 100, 3463–3471, 1995.

Neutsch, W. and Fahr, H. J.: The magnetic and fluid environment of an ellipsoidal circumstellar plasma cavity, Mon. Not. R. Astron. Soc., 202, 735–752, 1982.

Nickeler, D. and Fahr, H. J.: Stationary MHD-equilibria of the heliotail flow, in: The Outer Heliosphere: The Next Frontiers, Proceedings of the COSPAR Colloquium, edited by: Scherer, K., Fichtner, H., Fahr, H. J., and Marsch, E., COSPAR Coll., 11, 57–60, doi:10.1016/S0964-2749(01)80011-1, 2001.

Nickeler, D. H.: MHD equilibria of astrospheric flows, Ph.D. thesis, Utrecht University, Utrecht, Netherlands, 2005.

Nickeler, D. H. and Fahr, H.-J.: Reconnection at the heliopause, Adv. Space Res., 35, 2067–2072, 2005.

Nickeler, D. H. and Fahr, H.-J.: 2D stationary resistive MHD flows: Borderline to magnetic reconnection solutions, Adv. Space Res., 37, 1292–1294, 2006.

Nickeler, D. H. and Karlický, M.: Are heliospheric flows magnetic line- or flux-conserving?, Astrophys. Space Sci. Trans., 2, 63–72, doi:10.5194/astra-2-63-2006, 2006.

Nickeler, D. H. and Karlický, M.: On the validity of ideal MHD in the vicinity of stagnation points in the heliosphere and other astrospheres, Astrophys. Space Sci. Trans., 4, 7–12, doi:10.5194/astra-4-7-2008, 2008.

Nickeler, D. H. and Wiegelmann, T.: Thin current sheets caused by plasma flow gradients in space and astrophysical plasma, Ann. Geophys., 28, 1523–1532, doi:10.5194/angeo-28-1523-2010, 2010.

Nickeler, D. H. and Wiegelmann, T.: Relation between current sheets and vortex sheets in stationary incompressible MHD, Ann. Geophys., 30, 545–555, doi:10.5194/angeo-30-545-2012, 2012.

Nickeler, D. H., Goedbloed, J. P., and Fahr, H.-J.: Stationary field-aligned MHD flows at astropauses and in astrotails. Principles of a counterflow configuration between a stellar wind and its interstellar medium wind, Astron. Astrophys., 454, 797–810, 2006.

Nickeler, D. H., Karlický, M., Wiegelmann, T., and Kraus, M.: Fragmentation of electric currents in the solar corona by plasma flows, Astron. Astrophys., 556, A61, 2013.

Nickeler, D. H., Karlický, M., Wiegelmann, T., and Kraus, M.: Self-consistent stationary MHD shear flows in the solar atmosphere as electric field generators, Astron. Astrophys., arXiv:1407.3227, in press, 2014.

Papadopoulos, K.: A review of anomalous resistivity for the ionosphere, Rev. Geophys., 15, 113–127, doi:10.1029/RG015i001p00113, 1977.

Parker, E. N.: The Stellar-Wind Regions, Astrophys. J., 134, 20–27, 1961.

Parnell, C. E., Smith, J. M., Neukirch, T., and Priest, E. R.: The structure of three-dimensional magnetic neutral points, Phys. Plasmas, 3, 759–770, 1996.

Sahai, R. and Chronopoulos, C. K.: The Astrosphere of the Asymptotic Giant Branch Star IRC+10216, Astrophys. J. Lett., 711, L53–L56, 2010.

Scherer, K. and Fichtner, H.: The Return of the Bow Shock, Astrophys. J., 782, 25, doi:10.1088/0004-637X/782/1/25, 2014.

Speiser, T. W.: Conductivity without collisions or noise, Planet. Space Sci., 18, 613–622, 1970.

Suess, S. T. and Nerney, S.: Flow downstream of the heliospheric terminal shock. I – Irrotational flow, J. Geophys. Res., 95, 6403–6412, 1990.

Swisdak, M., Drake, J. F., and Opher, M.: A Porous, Layered Heliopause, Astrophys. J. Lett., 774, L8, doi:10.1088/2041-8205/774/1/L8, 2013.

Ueta, T.: Cometary Astropause of Mira Revealed in the Far-Infrared, Astrophys. J. Lett., 687, L33–L36, 2008.